Multiple Channel Interferometer for Metrology

C. R. Pond, M. H. Horman, and P. D. Texeira

A multiple channel interferometer was developed and used for the remote monitoring of the dynamic behavior of a large-diameter antenna experiencing simulated solar irradiance in a space simulation chamber. Reversible fringe-counting techniques were employed to measure changes in the distance between the equipment located outside the chamber and each of seven optical retroreflectors mounted on the face of the antenna. After the initial measurement program was completed, the equipment was modified to improve its performance.

Introduction

A multiple channel interferometer was developed to monitor the dynamic behavior of a large-diameter microwave antenna under test in a simulated space thermal and vacuum environment. Line-of-sight displacement measurements were made to seven small corner cube retroreflectors mounted on the face of the antenna. The measurements were made through a port in the space simulation chamber. The instrument was mounted on the outer wall of the chamber at a distance of about 5 m from the antenna. This paper describes the initial configuration of the instrument (developed on a short time schedule to make the required measurements) and subsequent improvements in the instrument. The test procedure and the instrument limitations are discussed.

Optical Configuration

The device is a modified multichannel Twyman-Green interferometer wherein the phase of the reference beam is modulated at 13.5 kHz to allow reversible fringe counting[1-3] in each channel. Each count corresponds to a distance increment of 7.9×10^{-6} cm (0.125 wavelength of the laser light). The optical configuration is shown in Fig. 1.

The beam from a 15-mW helium–neon (632.8-nm) laser is spatially filtered and collimated to a 5-cm diam beam. This beam is amplitude-divided into two beams (a reference beam and a signal beam) of equal amplitude. The reference beam is reduced to a 1.25-mm diam beam by a lens/microscope objective so it can pass through a Pockels cell. It is then reflected by a plane mirror and returned by the same path to the beam splitter. The optical path through the Pockels cell is varied at a 13.5-kHz rate to produce phase modulation of the optical carrier frequency. The double pass through the Pockels cell reduces the high voltage required in the modulator, since it doubles the phase shift obtained with a given Pockels cell voltage.

An aperture plate separates the signal beam into seven small beams, or pencils—one in the center and six evenly spaced around it. The pencils are 7 mm in diameter. Each of the seven signal beams passes through an adjustable delay line produced by a pair of right-angle prisms and a porro prism. These delay lines allow adjustments in the lengths of the signal paths in accordance with the coherence properties of the laser.[4] The signal beams and the reference beam interface produce high visibility fringes when their path lengths do not differ by more than 10 cm from an even multiple of the laser length. Each of the seven signal pencils is reflected to its respective 3-mm diam corner cube retroreflector[5,6] by an adjustable mirror. The beams are reflected back upon themselves by the retroreflectors and retrace their paths to the beam splitter. The signal pencils are larger than the retroreflectors to permit some lateral motion of the corner cubes. The light scattered into the output arm of the interferometer is limited by the previously mentioned aperture plate in the signal beam and by a pinhole aperture in the reference beam. In addition, the delay lines are turned about 10° from normal to the incident beam so that the first surface reflections of the right-angle prisms will not illuminate the detectors. The output arm also has an array of seven 7-mm diam apertures. Each aperture passes a beam returned from a retroreflector and a portion of the reference beam to a detector. Interference between these two beams produces variations in the light intensity on the detector.

The authors are with Boeing Aerospace Group, P.O. Box 3999, Seattle, Washington 98124.

Received 26 January 1971.

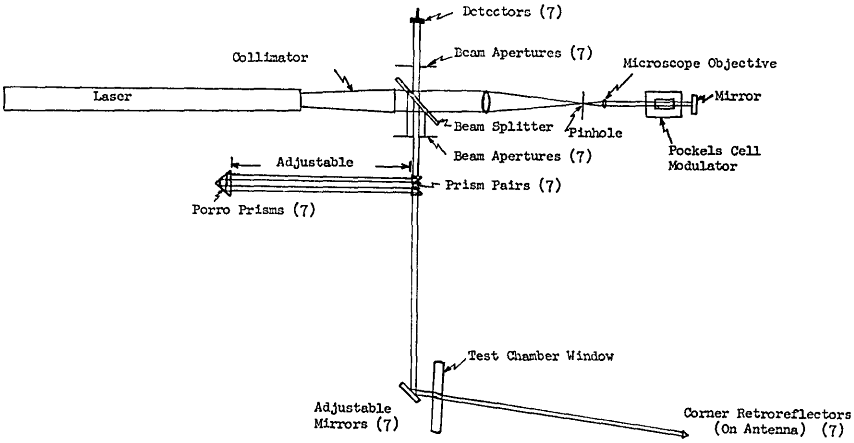

Fig. 1. Optical configuration of multiple channel interferometer.

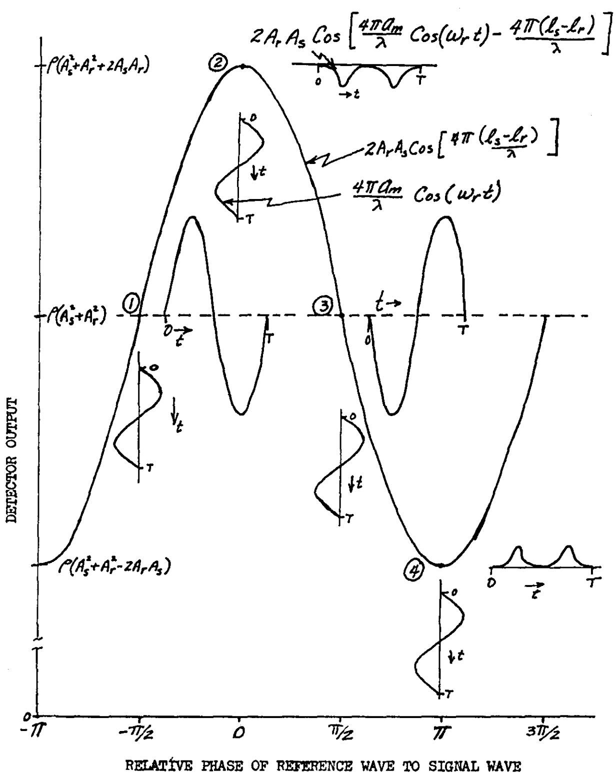

Fig. 2. Modulation diagram.

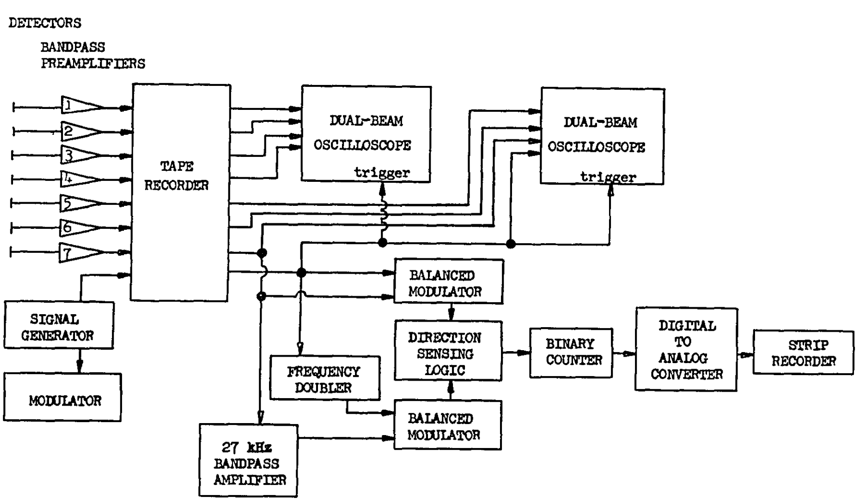

Fig. 3. Electronics block diagram.

Basis for the Signal Processing

The output voltage across each detector varies as a function of the signal path length and the phase modulation introduced by the modulator. Let the amplitude variation of the signal beam wavefront incident on a detector be $A_s \exp\{i\,[\omega_c t + (4\pi/\lambda)L_s]\}$, where A_s is the peak amplitude, $\omega_c = 2\pi f_c$ where f_c is the optical carrier frequency, L_s is the optical path length from the beam splitter to the retroreflector along the signal path, t is time, and λ is the wavelength of the laser light. Let the amplitude variation of the reference beam be $A_r \exp\{i\,[\omega_c t + (4\pi/\lambda)L_R + a_m \cos \omega_m t]\}$, where A_r is the peak value of the amplitude, L_r is the optical path length from the beam splitter to the mirror in the reference path, a_m is the amplitude of the phase modulation, and $\omega_m = 2\pi f_m$ where f_m is the modulating frequency (13.5 kHz).

The output $E_D(t)$ of the detector, being proportional to the intensity of the incident wavefronts (the square of the vector sum of the incident wavefront amplitudes), is given by

$$E_D(t) = \rho\big(A_s^2 + A_r^2 + 2A_rA_s \cos\{a_m \cos(\omega_m t) - 4\pi(L_s - L_r)/\lambda\}\big),$$

where ρ is the responsivity of the detector.

This equation can be expressed in terms of a fourier series[2] as shown below:

$$E_D(t) = \rho \left\{A_s^2 + A_r^2 + 2A_sA_r \left[{}^1\!/_2 A_0 + \sum_{n=1}^{\infty} A_n \cos(n\omega_m t)\right]\right\},$$

where $A_n = 2J_n(4\pi a_m/\lambda) \cos\{[4\pi(L_s - L_r)/\lambda] - (n\pi/2)\}$ for $n = 0, 1, 2, \ldots$. Figure 2 is a physical picture of how a detector's output voltage $E_D(t)$ varies as a function of the phase modulation for specific values of $(L_s - L_r)/\lambda$ (i.e., the relative phase of the reference wave and the signal wave). The large sine wave represents the detector output voltage as a function of signal path length in the absence of modulation. The small sine waves on vertical axes represent phase modulation introduced in the reference beam. The more complex waves on small horizontal axes are the detector output signals. Note that at points *1* and *3* the phase modulation produces a detector output voltage variation having the same frequency as the modulating frequency but differing by 180° in phase. The modulation at points *2* and *4* results in detector output variations having twice the modulating frequency but differing by 180° in phase. Thus, there is an ordered sequence of four conditions relative to the phases of the reference voltages: (1) fundamentals 180° out of phase, (2) second harmonics 180° out of phase, (3) fundamentals in phase, and (4) second harmonics in phase. This sequence allows an unambiguous determination of whether the signal path length has increased or decreased in quarter-fringe increments.

Electronics

A block diagram of the electronics required to process the signals previously described is shown in Fig. 3. The outputs of the photodetectors are applied to identical bandpass amplifiers. The amplifier response characteristic rolls off at 31 kHz on the high frequency end and at 9.5 kHz on the low frequency end. The amplifier response below 200 Hz is more than 60 dB below the midfrequency response. This eliminates the effects of the simulated sun and other extraneous lighting. The amplifier gain is manually adjustable and of sufficient magnitude to drive the tape recorder used for the measurements. (Recording the signals was necessary because the electronics for processing only one channel were available.)

During the test, the output from one channel was processed in real time. The outputs of the tape recorder were monitored on two Tektronix dual-beam oscilloscopes to ensure that all seven signals and reference were being recorded. These same displayed signals were used to determine and maintain adjustment of the system optics.

The processing circuitry operates as follows: The output of a bandpass amplifier (or tape recorder channel) contains a 13.5-kHz and 27-kHz phase and amplitude-modulated signal. Since the magnitude of the 27-kHz signal is about 20 dB below the 13.5-kHz signal, the signal from the bandpass amplifier (or tape recorder) is applied to another bandpass amplifier with a center frequency of 27 kHz and a bandwidth of ± 4 kHz. This bandpass amplifier increases the amplitude of the 27-kHz signal to the same level as the 13.5-kHz signal.

Two balanced modulators serve as phase detectors to derive the phase quadrature signals needed to determine whether the optical path length is increasing or decreasing. One balanced modulator uses the 13.5-kHz signal and a 13.5-kHz reference voltage, the same signal that drives the electrooptical modulator. The input to the other balanced modulator is the 27-kHz signal and a 27-kHz reference voltage of constant amplitude and phase. The latter is obtained by full wave rectification of the modulator driver voltage. This rectified signal has a strong 27-kHz frequency component and no 13.5-kHz frequency component. It is then filtered by a very narrow bandpass filter having a center frequency of 27 kHz.

The balanced modulator output of interest, after filtering by a low pass filter, is given by $A_s(t) \cos(\phi_s - \phi_r)$, where $A_s(t)$ is the amplitude of the signal as a function of time and $(\phi_s - \phi_r)$ is the phase difference between the signal and the reference. As previously described, the phase difference is either 0° or 180°; therefore, $\cos(\phi_s - \phi_r)$ can be replaced by ± 1.

The balanced modulator outputs are shown in Fig. 4. The graphs show the phase and amplitude variation as a function of optical path length. Note that phase quadrature exists between the outputs of the two balanced modulators. This property of the two outputs enables the direction-sensing logic to make unambiguous direction determination. These sinusoidal waveforms are then modified by the shaping circuitry.

The rectangular function shown in Fig. 5 is the output of the shaping circuitry for the frequency compo-

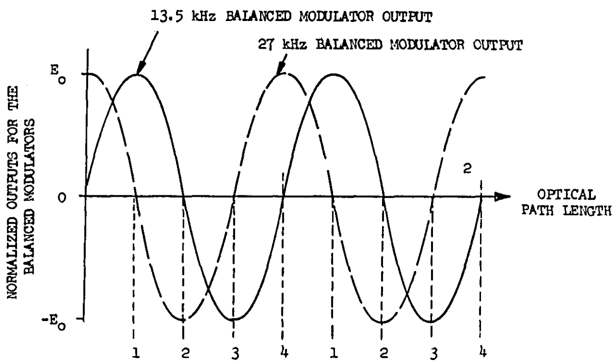

Fig. 4. Phase comparison between the outputs of the balanced modulators.

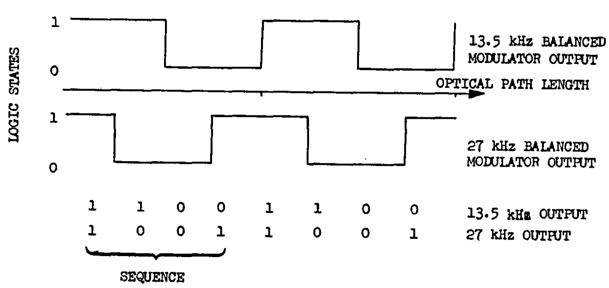

Fig. 5. Logic representation of the balanced modulator output.

nents of interest. The lower part of Fig. 5 shows the logic states assigned to the output of the shaping circuits. Four distinct states result for each wavelength of change in optical path length. The direction-sensing logic compares the present state and the preceding state to determine whether the path length is increasing or decreasing.

The direction sensing logic has two output terminals, one for an increase in path length and the other for a decrease in path length. A pulse from either output represents a quarter-wavelength change in optical path length. These pulses are inputs for a fifteen-bit reversible binary counter which drives a fifteen-bit digital to analog converter. The analog voltage output from the digital to analog converter is proportional to the change in path length.

Test Procedures and Data Reduction

Figure 6 is a photograph of the interferometer mounted on the side of the space simulation chamber in the Boeing Space Center in Kent, Washington. Figure 7 is a photograph of the entire instrument and associated equipment as used during the measurements. The chamber port can be seen behind the pointing mirror array. Although the angular *substence* of the retroreflectors on the antenna (as viewed through the port) was less than a milliradian, the retroreflectors were readily located by holding a flashlight close beside one's eye and shining the beam on the antenna. Light from

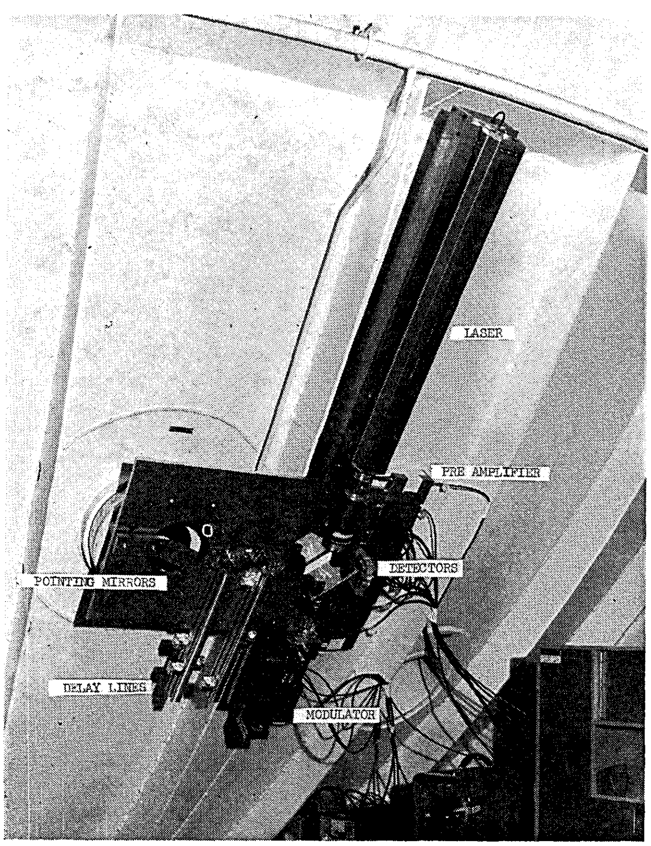

Fig. 6. Multiple channel interferometer optics.

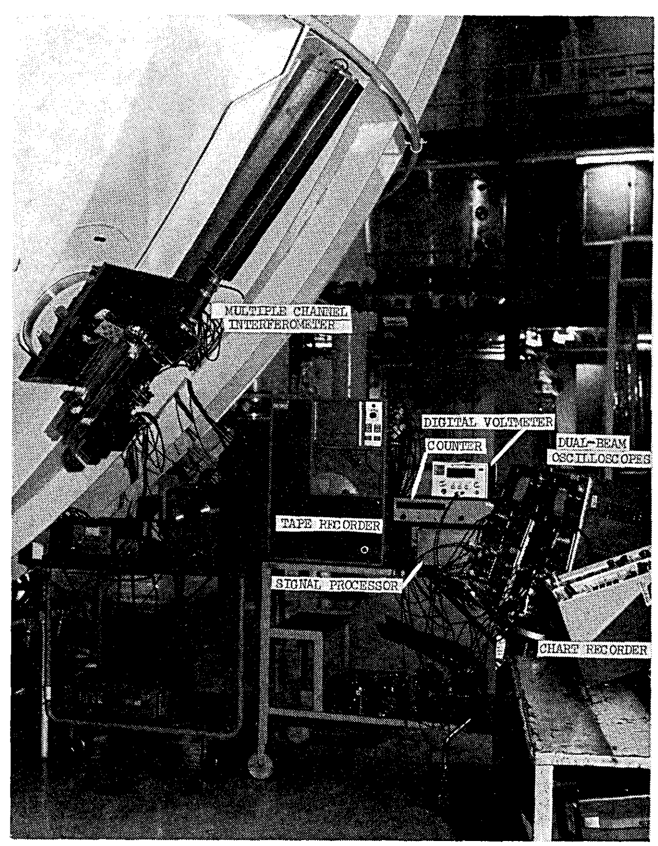

Fig. 7. Quartz antenna measuring equipment.

the laser beams could be seen reflecting from the white face of the antenna. When a beam was directed onto a corner reflector, a bright red return could be seen. Thus pointing the laser beams was very easy. The detector outputs displayed on the oscilloscopes also gave an indication of the alignment of the laser beams on the retroreflectors. These displays were used to adjust the beam directions to peak up the returns.

The oscilloscope patterns were also used to adjust the lengths of the optical delay lines for high contrast interference signals. The best signal-to-noise ratios were obtained when the signal arm was precisely a multiple of twice the laser length difference in length from the reference arm. Even a small variation from an optimum length would produce a marked increase in the laser noise. Small variations also degraded the fringe contrast obtainable, although the signals were usable for variations up to about 5 cm. During static situations, with the interferometer measuring the changes in optical path to an object mounted on its own support structure some 5 m away, the counter output may be observed to vary due to building vibrations and air motions in the path. The mean value of the counter does not vary.

The Pockels cell phase modulation technique was the greatest source of problems, of which the major ones were the following:

(1) The birefringent effects of the Pockels cell modulator could not be eliminated over the entire beam aperture. The residual polarization modulation caused some amplitude modulation in all but one of the signal channels.

(2) Extraneous noise resulted from light reflected and scattered from the microscope objective, the Pockels cell faces, and so on.

(3) The interference pattern at the detector plane displayed a fringe movement reminiscent of a heat wave. The cause of this was not determined although the source of the disturbance was in the reference arm. It is suspected that an index of refraction matching oil in the Pockels cell was producing the effect due to nonuniform heating.

(4) During the measurements there was not enough second harmonic phase modulation introduced. This resulted principally from a misconception of the appropriate signal waveform.

The results were not repeatable during the initial phase of the data reduction process. The oscilloscope signals—which were triggered by the recorded modulator signal—were seen to move back and forth. This was caused by wow and flutter in the tape recording which introduced large phase errors between the signals recorded on the various channels. Consequently, the recorder reference signal could not be used to generate the 13.5-kHz and 27-kHz reference voltages.

Additional circuitry was developed to supply the necessary reference voltages. The 27-kHz reference voltage was derived from the 13.5-kHz signal voltage by full wave rectification and filtering. Although the 13.5-kHz signal exhibits two conditions of phase (a phase difference of 180°) and amplitude fluctuations, full wave rectification produces a strong 27-kHz frequency of constant phase but varying amplitude. The narrow band bandpass filter utilized was a multiplier which removed the extreme amplitude fluctuations, providing a reference of nearly constant phase and amplitude. The 13.5-kHz reference voltage was derived by dividing the 27-kHz reference by 2.

Modified Optical Configuration

The optical configuration has undergone several modifications since the first measuring program. Since the diagrams of the new configurations would be very similar to Fig. 1, the changes will be briefly described.

First, the electrooptical modulator was replaced by a piezoelectric bender. A small mirror fleck was cemented to one of the bender's faces to reflect the reference beam. This mirror was located at the focal point of the lens in the reference beam. The advantages of the bender in this application are (1) the high voltage requirements are eliminated (the bender can be driven by the output of the signal generator), (2) a greater phase variation is easily obtained to produce greater depth of modulation, and (3) there is no polarization modulation of the reference beam produced by this modulator.

The second modification was the installation of a plane-parallel optical flat in the signal beam. Rotating this flat through a preset angle introduces a known change in the optical path length of all seven beams. This feature allows a simple check on the operation of all of the channels.

The third modification was the replacement of the laser by a single-frequency laser (Spectra-Physics Model 119) and the removal of the optical delay lines. This laser operates with a much lower optical power (0.2 mW) but provides adequate signal-to-noise ratios at the detectors. One problem introduced by the new configuration was optical feedback into the laser. Normally this would be corrected by using an optical isolator at the output of the laser and a second beam splitter to compensate for polarization changes; however, this solution introduced too much loss in the system. The feedback was reduced to an acceptable level by introducing apertures in the reference arm to eliminate all the light not required for the system's operation. This not only decreased the amount of light in the reference beam but also reduced the fraction of the light that could get back through the pinhole in the beam cleaner, since the diffraction patterns of the light coming through the apertures are much larger than that of the original reference beam.

Modified Electronics

Figure 8, a schematic of the modified electronic circuitry, shows that all the channels have been instrumented to allow the data to be reduced during the measurements. One additional circuit was required to allow phase adjustment between the signal generator and the processing electronics. This adjustment corrects for the phase difference between the signal driving

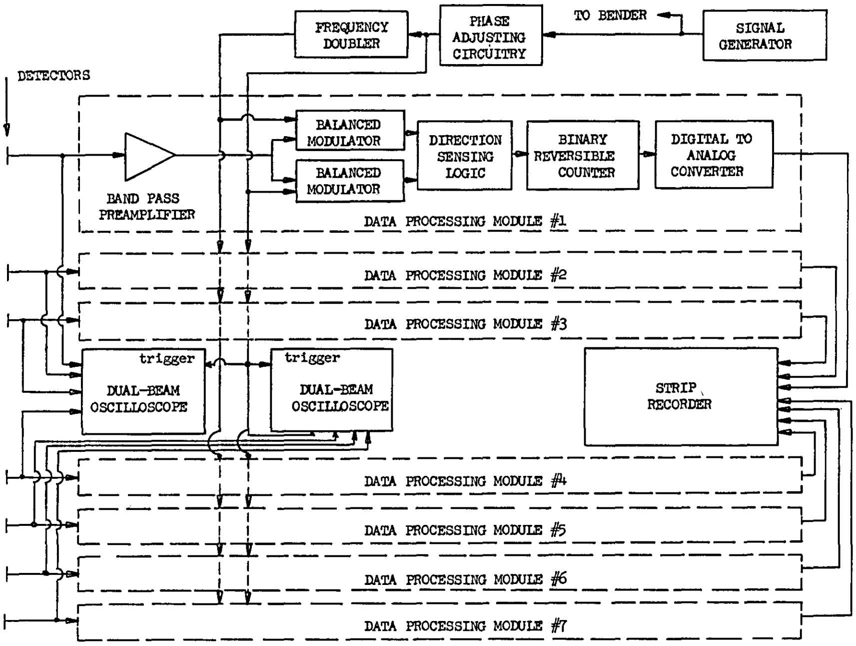

Fig. 8. Modified electronics block diagram.

the bender and the actual change in path length produced by the bender.

This paper was presented at the Spring meeting of the Optical Society of America, 7 April 1970, in Philadelphia.

References

1. E. R. Peck and S. W. Obetz, J. Opt. Soc. Am. **44**, 505 (1953).
2. H. A. Deferrari and F. A. Andrews, J. Acoust. Soc. Am. **39**, 979 (1966).
3. H. A. Deferrari, R. A. Darby, and F. A. Andrews, J. Acoust. Soc. Am. **42**, 982 (1967).
4. A. G. Fox and T. Li, Bell Syst. Tech. J. **40**, 453 (1961).
5. E. R. Peck, J. Opt. Soc. Am. **38**, 1015 (1948).
6. M. V. R. K. Murty, J. Opt. Soc. Am. **54**, 1187 (1964).

Anders K. Ångström (left) receiving the IMO prize for 1962 from A. Viaut (then President of the World Meteorological Organization) during a ceremony in the Swedish Foreign Office in Stockholm.